

# DeepThin: A Self-Compressing Library for Deep Neural Networks

Matthew Sotoudeh\*  
Intel/UC Davis  
masotoudeh@ucdavis.edu

Sara S. Baghsorkhi  
Intel  
sara.s.baghsorkhi@intel.com

## Abstract

As the industry deploys increasingly large and complex neural networks to mobile devices, more pressure is put on the memory and compute resources of those devices. Deep compression, or compression of deep neural network weight matrices, is a technique to stretch resources for such scenarios. Existing compression methods cannot effectively compress models smaller than 1-2% of their original size. We develop a new compression technique, DeepThin, building on existing research in the area of low rank factorization. We identify and break artificial constraints imposed by low rank approximations by combining rank factorization with a reshaping process that adds nonlinearity to the approximation function. We deploy DeepThin as a plug-gable library integrated with TensorFlow that enables users to seamlessly compress models at different granularities. We evaluate DeepThin on two state-of-the-art acoustic models, TFKaldi and DeepSpeech, comparing it to previous compression work (Pruning, HashNet, and Rank Factorization), empirical limit study approaches, and hand-tuned models. For TFKaldi, our DeepThin networks show better word error rates (WER) than competing methods at practically all tested compression rates, achieving an average of 60% relative improvement over rank factorization, 57% over pruning, 23% over hand-tuned same-size networks, and 6% over the computationally expensive HashedNets. For DeepSpeech, DeepThin-compressed networks achieve better test loss than all other compression methods, reaching a 28% better result than rank factorization, 27% better than pruning, 20% better than hand-tuned same-size networks, and 12% better than HashedNets.

DeepThin also provide inference performance benefits in two ways: (1) by shrinking the application working sets, allowing the model to fit in a level of the

cache/memory hierarchy where the original network was too large, and (2) by exploiting unique features of the technique to reuse many intermediate computations, reducing the total compute operations necessary. We evaluate the performance of DeepThin inference across three Haswell- and Broadwell-based platforms with varying cache sizes. Speedups range from 2X to 14X, depending on the compression ratio and platform cache sizes.

## 1 Introduction and Motivation

In recent years, machine learning algorithms have been increasingly used in consumer-facing products, such as speech recognition in personal assistants. These algorithms rely on large weight matrices which encode the relationships between different nodes in a network. Ideally, these algorithms would run directly on the client devices such as Amazon Echo [20] and Google Home [14], which utilize them. Unfortunately, because such devices are usually portable, low-power devices, running such expensive algorithms is infeasible due to the significant storage, performance, and energy limitations involved.

To work around this problem, many developers have resorted to executing the inference models on high-performance cloud servers and streaming the inputs and outputs of the model between client and server. This solution, however, introduces many issues, including high operational costs, use of large amounts of data transfer on metered (mobile) networks, user privacy concerns, and increased latency.

Recent research has investigated methods of compressing models to sizes which can be efficiently executed directly on the client device. Such compression approaches must reduce the model space requirement without significantly impacting prediction accuracy, runtime performance, or engineering time. Our work builds on existing research in the area of low rank factorization. We develop a new compression method and library, DeepThin, that:

---

\*Work done while at Intel.

1. Solves the fundamental symmetry issue with extremely low-rank matrix factorization of machine learning model parameters, using an auxiliary intermediate matrix and an efficient re-layout operation.
2. Is integrated with the popular and commonly used TensorFlow framework, enabling users to seamlessly compress models at different granularities. We also implemented previous work compression techniques in our library to compare accuracy loss across compression methods.
3. Consistently results in better accuracy at the same size as the previous compression methods.
4. With our customized C++ TensorFlow operations built on top of MKL [11], empirically demonstrates inference performance speed-ups from 2X to 14X over uncompressed models.

## 2 Related Work

One of the most successful approaches for reducing the total number of free parameters in a network is iterative pruning [9]. A large network is initially trained, then the subset of connections with magnitude closest to 0 are removed. This train-prune cycle is repeated until the network reaches a desired size and accuracy. Han et al. show iteratively pruned models can compress up to 13X with no loss of accuracy [9]. Iterative pruning, however, is less than ideal in practice.

First, there is no way of storing the pruned network that fully realizes the reduction in free parameters. Common storage methods for sparse matrices, including compressed-sparse-row and -column formats [19], more than double the actual stored size of the network when compared to the number of free parameters. CSR, for example, stores sparse matrices as a combination of three vectors - two of which hold one element for each non-zero element in the matrix. Thus, a network pruned to  $\frac{1}{N}$  of its original number of free parameters will be more than  $\frac{2}{N}$  of its original size once it is actually stored in CSR form.

Furthermore, pruning works by taking advantage of the fact that the vast majority of weights in a network are unimportant to the final output. After removing all of those weights, however, further pruning forces the network to remove increasingly important connections. This causes highly-pruned models to lose accuracy rapidly and, empirically, limits the effectiveness of pruning when targeting compressed sizes significantly smaller than  $\frac{1}{50}$  of the original model.

Finally, pruning networks introduces many hyperparameters (such as the intervals at which to prune and the exact saliency algorithm to use [16]), optimization of which can have positive effects on compressed model accuracy but require significant hand-tuning during the training process. Often this effort is not worth the additional accuracy gains, leaving many pruned models with remaining inefficiency.

Alternatively, success has been found by reducing the bit width of and quantizing the network weights [8]. However, lowering bit widths imposes a large lower bound on the compressed size (after which weights are represented by single bits and cannot be quantized further).

Better encoding methods, particularly Huffman [10] and run-length coding, can build on quantized weights to achieve significantly smaller file sizes [8]. Unfortunately, such techniques rely on the actual distribution of trained weights in a network, making it impossible to accurately predict model sizes until training is complete. This limitation is often unacceptable in practice, when one wishes to train a model for specific size requirements. Additionally, such methods require significant overhead during the layer computation (as they must decode each individual weight), further degrading model performance.

HashedNetworks are similar to weight quantization and clustering, except the assignment of weight to cluster is determined according to a hash function (so only the cluster means, and not the weight-cluster mapping, need to be stored) [4]. Essentially, each element of the weight matrix is chosen at computation time from a vector of possible values according to the hash of its row and column indices.

Such HashedNets require the computation of a hash function for each weight in the network, adding significant computational complexity to a model. Furthermore, they rely on random memory access patterns which are particularly difficult to optimize for. Finally, because weights are shared randomly in a layer, it is difficult for HashedNetworks to learn logical local patterns in data (which are particularly present in speech, image, and other continuous data).

Recently, Ha et al. introduced HyperNetworks, which use a small "internal" network to generate the weights for the main "outer" network [7]. Ha et al. focus on the power of such HyperNetworks to change their weights over time, but the method also has significant compression potential. However, they hand-designed different,

complex internal networks for each class of model, making it more difficult to apply their research to new model architectures without significant engineering overhead.

Finally, Denil et al. and others have shown that weight matrices may be factored into smaller matrices at training time to aid in distributed model training [6, 13, 18]. Conceptually, weight factorization can be thought of as a special case of the HyperNetwork idea, where the “internal” network is represented by a simple multiplication of the two matrix factors. Unfortunately, Denil et al. were unable to effectively train both of the factored weight matrices at once, and instead relied on a pretraining scheme to fix the values of one of the factored matrices before training. These pretrained matrix values, while not needing to be further trained, are not efficiently distributable, significantly limiting the technique’s effectiveness beyond improving training efficiency on distributed systems. Additionally, they did not provide a means of further training the initialized matrix values, which should theoretically result in improved accuracy.

This paper builds on the weight factorization design, improving on and empirically testing it in many important ways to get our “DeepThin” compression method. In addition, we provide empirical and theoretical best practices for using DeepThin.

### 3 DeepThin Compression Model

Standard deep neural networks consist of conceptual “layers” chained one after another, through which input data passes sequentially until finally reaching a desired output. Each layer computes a matrix multiplication between the outputs of the previous layer and the current layer’s weight matrix. After computing the matrix multiplication, bias terms are added and a non-linear activation function is applied to the output.

For data with some time dependency, recurrent neural networks (RNNs) can be used. Although there are different types of RNNs, they all involve a model containing a number (usually three or four) of compute steps similar to the one described above. Such models can be more parameter-efficient than regular DNNs, but they still require prohibitively large weight matrices to achieve useful levels of accuracy and thus also benefit greatly from compression methods.

For visual data, convolutional neural networks (CNNs) sweep learned filter banks (weights) over the input data to extract common features. Each sweep step is computationally similar to the layer operation described

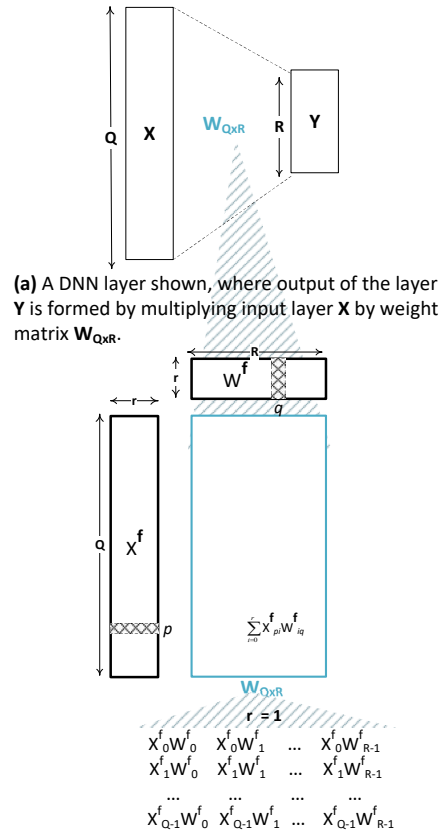


**Figure 1.** Lower rank factorization of a weight matrix: as  $r$  becomes smaller, rows and columns of the reconstructed matrix start to become more of a scaled version of each other.

above. That said, because the size of input and output buffers in current state-of-the-art convolutional networks represent an unusually large percent of actual network memory requirements (due to large number of input/output channels), in this work we mainly focus on RNNs and feed forward DNNs. Nevertheless, there is no fundamental limitation to apply DeepThin compression method to CNNs.

Throughout this work we apply the compression methods to each layer’s weight matrix independently. A single layer with a non-linear activation function  $a$ , weights  $W$ , and biases  $B$  is defined as:

$$Y = a(X.W + B) \quad (1)$$

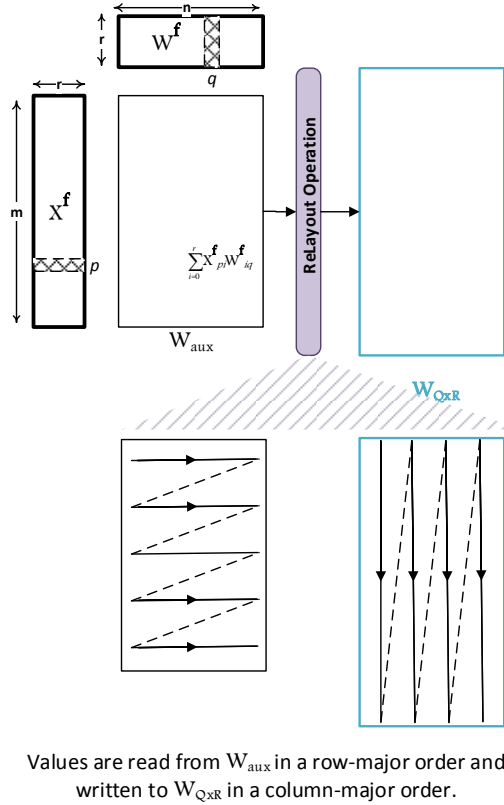


**Figure 2.** Breaking the artificial structural constraint created by factorization. This transform has two learnable parameters: low rank factors  $X^f$  and  $W^f$ .

, where  $W$  and  $B$  are learnable parameters that must be stored within the network. As the size of  $B$  is often negligible compared to  $W$ , we only consider here compression of the  $W$  parameter (although we do compress the biases in our evaluations).

The DeepThin architecture proposed in this paper can compress (with some loss of accuracy) any model that relies on storing large weight matrices such as  $W$  in Equation 1.

## 4 DeepThin Architecture

In this section we introduce our compression approach and show how it evolved from a low-rank approximation method.

Rank factorization compression algorithms work by replacing the weight parameter  $W$  in Equation 1 with a function of a smaller set of learnable parameters [6, 7, 18]. For example, in rank approximation as shown in Figure 1, a  $Q \times R$  weight matrix  $W$  is represented as the product of two lower rank matrices:

$$W_{Q \times R} \approx X^f \cdot W^f \tag{2}$$

where  $X^f$  is a  $Q \times r$  matrix and  $W^f$  is an  $r \times R$  matrix. During training, the error signal is back-propagated to the low rank factors  $X^f$  and  $W^f$  to update their elements the same way a regular weight matrix is trained. The learned factors are then used to reconstruct the weight matrix at each layer during the forward training or inference passes. Lower rank factorizations of a weight matrix – specifically when  $r$  equals 1 – are more appealing from both a storage and computational efficiency standpoint. But as  $r$  becomes smaller, rows/columns of the reconstructed weight matrix begin to resemble each other. In the bottom part of Figure 1 we show that, for  $r=1$ , every set (row) of weights generated by the low rank approximation is a semi-scaled copy of the weight vector  $W^f$ , and all columns are a scaled copy of the vector  $X^f$ . Unfortunately, we have found that this artificial resemblance considerably impacts the learning performance and capacity of a network by requiring all output nodes in a layer to recognize very similar input patterns (introducing extreme redundancy).

To reduce the negative impact that such artificial constraints have on network learning capacity, DeepThin first applies rank approximation to an auxiliary matrix  $W_{aux}$  of size  $m \times n$ .

$$W_{aux} = X^f \cdot W^f \tag{3}$$

where now  $X^f$  is a  $m \times r$  matrix and  $W^f$  is an  $r \times n$  matrix.

Next, elements of  $W_{aux}$  are redistributed into  $W_{Q \times R}$  such that the artificial symmetry is broken. The reshaping process adds non-linearity to the approximation function the same way an activation function adds a nonlinear decision boundary to the network’s output layer. On first glance, an ideal nonlinear transfer function would randomly scatter elements of matrix  $W_{aux}$  into matrix  $W_{Q \times R}$ . We performed tests with that scattering as a limit study, and as expected found that it was extremely slow (due primarily to the random memory accesses involved). Furthermore, such a scattering scheme requires a matrix of indices to relate the original position to the re-laid-out position, which undermines the compressibility.

A more cost-effective alternative would be to distribute rows of  $W_{aux}$  along columns of  $W_{Q \times R}$  as shown in Figure 2. Note that this differs from a simple transpose in that one column of  $W_{Q \times R}$  may be composed of multiple (or only part of a) row of  $W_{aux}$ .

This reshaping is especially appealing when computing a matrix multiplication because it constructs a column (or part of a column) of  $W_{Q \times R}$  at a time, in an array of consecutive memory location, while multiplying them by different rows of input matrix  $X$  in Equation 1. Thus, it makes full use of the generated elements before discarding them.

Additionally, and to our surprise, we have found that reshaping with this method often achieves better accuracy than with the random scatter method. See Figures 4 and 6 for a comparison between DeepThin and the random scattering (DeepThin Shuffled). We hypothesize that this is due to the random scattering not being able to take advantage of local patterns in the data and weight matrices. Thus, we find that there may be some trade-off between allowing the network to take advantage of such local patterns and getting "stuck" by forcing the usage of such patterns as rigidly as in the simple factorization approach.

Nevertheless, the above reshape function may still result in repetition patterns in matrix  $W_{Q \times R}$  in form of blocks (of columns) scaled slightly differently. To solve this problem, it is important in practice to choose the number of columns in matrix  $W^T$  to be prime with respect to the number of rows in matrix  $W_{Q \times R}$ . In other words, we prefer to have:

$$\text{LCM}(n, Q) = n \times Q \quad (4)$$

where LCM is the least common multiple of the two numbers. The LCM value determines the repetition frequency of similar, scaled blocks in matrix  $W_{Q \times R}$ . Here  $Q$ , the original weight matrix width, is fixed. So, ideally we must choose the largest value for  $n$  that is prime with respect to  $Q$ . But parameter  $n$  must also satisfy other constraints within the DeepThin compression framework. First, matrix  $W_{\text{aux}}$  needs to have at least as many elements as matrix  $W_{Q \times R}$ . Therefore:

$$m \times n \geq Q \times R \quad (5)$$

In addition, DeepThin parameters need to abide by the specified compression rate. Because DeepThin compresses weights on a per-matrix basis, we can calculate the compressed size of any individual compressed matrix in the network. Therefore, for a compression ratio of  $\alpha$  and a weight matrix of shape  $Q \times R$  we have:

$$\alpha = \frac{r \times (m + n)}{Q \times R} \quad (6)$$

where the denominator totals the size of the weight matrix  $W_{Q \times R}$ , and the numerator sums up the size of low rank factors of matrix  $W_{\text{aux}}$ . Note that we do not include the size of the bias vector in this calculation. In practice, we compress and compute the bias vector's compression rate separately if required by the user. Again, note that Equation 6 ignores other, much smaller parameters of the network that are not compressed (such as batch-normalization [12] parameters), thus the actual network size will have some overhead. If the exact network architecture is known, one may add those other parameters to Equation 6 to get an exact ratio for the entire network or to further compress the other parameters to reach a desired overall compress rate. Our library automatically compensates for these parameters, but for ease of explanation we maintain the simple form of Equation 6.

Now, if we replace  $m$  in Equation 6 with its lower bound value derived from Inequality 5, for each rank factorization value ( $r = 1, r = 2, \dots$ ), we have a single variable quadratic inequality as shown below:

$$\alpha \geq \frac{r \times \left( \frac{Q \times R}{n} + n \right)}{Q \times R} \quad (7)$$

for which valid ranges of  $n$  can be easily determined if any exist. Within valid ranges, we then pick a minimum value of  $n$  that satisfies conditions expressed by Equations 5 and 4. Since this fine tuning only happens once during initialization of the network the performance overhead is negligible.

Non-existence of a valid range for  $n$  in Inequality 7 indicates that the spatial overhead of DeepThin surpasses any compression benefit it provides for the specific matrix being compressed. This creates an effective lower-bound on the compression rate  $\alpha$  supported by DeepThin. This lower-bound is dependent on the size of the original network weight matrix  $W_{Q \times R}$  but is often less than  $\frac{1}{1000}$  of the matrix size.

Additionally, different matrices in a network may have different shapes and thus different lower bounds. This makes it often possible to over-compress larger matrices in order to "make up for" matrices that have hit this lower bound, thus achieving a desired overall compressed network size (see Section 5.3 for our library's approach to this).

#### 4.1 Similarities to a Single-Layer Neural Network

Conceptually, the DeepThin architecture can be thought of as an inner, single-layer neural network that generates the weights for the larger outer network layer (akin to a HyperNetwork). This single-layer “internal” network does not include a bias or activation function, though it benefits from nonlinearity added via the re-layout transformation. Although biases serve an important role in standard network layers, allowing the network to effectively shift the activation function, our “internal” networks do not need such biases for multiple reasons. First, values in  $W^f$  and  $X^f$  are distributed around a mean of 0. So any biases added to the output of the DeepThin transform would determine the expected mean of the generated weights  $W_{Q \times R}$ . Because original network weights,  $W_{Q \times R}$ , are almost always centered about 0, removing the biases from the internal network does not affect accuracy. Additionally, because we do not have activation functions on the “internal” network, biases do not provide the “function-shifting” benefit. Activation functions, on the other hand, have squashing effects that may limit the range of values generated for the reconstructed matrix  $W_{Q \times R}$  – a new set of artificial constraints that may impact the learning capacity of the original network.

Single-layer internal networks have many benefits, including requiring very little engineering and better compute efficiency at runtime. Nevertheless, a natural question is whether a deeper model could help better reconstruct matrix  $W_{Q \times R}$ , and improve the compressed network’s accuracy.

Ideally, one should be able to extend the DeepThin architecture such that lower rank factor matrices –  $X^f$  and  $W^f$  in Figure 2 are themselves recursively lower-rank approximated and reshaped within another inner DeepThin layer. The premise here is that only the innermost layer’s thinner rank factor matrices are learned and stored with the hope that they can reconstruct much larger weight matrices on the fly for the outermost DeepThin layer(s), resulting in lower loss of accuracy.

We performed experiments with such extensions of DeepThin, and were able to show an experimental accuracy improvement of up to only about 1%. This soon hits the point of diminishing returns, as deeper internal networks become significantly more difficult to optimize for (particularly taking into account the size of intermediate buffers that would need to be preserved).

Therefore, in the rest of the paper, we focus on the single layer DeepThin architecture. In Section 6 we show that the single-layer DeepThin performs very well, almost always beating other compression methods.

## 5 DeepThin Library Implementation

We implement DeepThin and previously proposed compression methods as library modules integrated with the open-source TensorFlow [2] framework. The TensorFlow framework first builds a graph of learnable variables and operations on those variables in Python. Next, the graph is evaluated on the compute device using platform-specific libraries. TensorFlow is capable of automatically differentiating complex graphs built with a standard set of operations included in TensorFlow. Furthermore, optimization algorithms included with TensorFlow can use automatically calculated gradients to iteratively optimize all the learnable variables on a graph, with the details of gradient computation and parameter updates abstracted from the user or other libraries.

### 5.1 Training

For training, instead of calling the standard TensorFlow library to declare learnable variables for each of the network’s weight matrices, the user calls a function in our library which mimics the TensorFlow API. Instead of declaring a single learnable variable node on the computation graph, our library creates a separate sub-graph for each variable, which may have its own learnable parameters (e.g.,  $X^f$  and  $W^f$ , for DeepThin-compressed matrices) and operations (re-layout operation defined in Section 4). The output of that sub-graph can then be used as a drop-in replacement for a regular learnable matrix in TensorFlow. Additionally, because we are able to express our operations as a combination of existing TensorFlow operations, TensorFlow is able to automatically derive the gradient computations and correctly backpropagate the error signal to the learnable parameters of the sub-graph ( $X^f$  and  $W^f$  for DeepThin).

For DeepThin-compressed models, the sub-graph consists of two learnable parameters,  $X^f$  and  $W^f$ , which undergo a matrix-multiplication, transposition, slice, and reshape in order to implement our re-layout operation.

The rank factorization sub-graph is simpler, where two factors  $X^f$  and  $W^f$  are multiplied and the result is

used in the rest of the graph. Note that the first dimension of  $X^f$  and the last dimension of  $W^f$  must match the respective dimensions of the requested matrix shape, a requirement that is not applied to DeepThin-compressed models, where the re-layout operation reshapes and slices the product matrix  $W_{aux}$  to the desired size.

HashedNet sub-graphs contain a learnable set of “hash bins”, then a fixed mapping from bins to locations in the uncompressed matrix  $W$  (which is determined by pre-computing the hash as described in the HashedNet paper[4] and source code). Finally, a gather operation is performed and the resulting  $W$  matrix is used in the model graph.

Pruned matrices are created by a sub-graph that consists of a learnable matrix and a “mask” composed of binary 0 and 1 values. The two are element-wise multiplied, and the resultant masked matrix is returned. The library user must place a call to our library’s “step” function within their training loop, to indicate that another training iteration has passed. At each training iteration, the library determines whether or not to prune the network at this step – determined by a user-configured pruning schedule. The mask starts off filled with 1s, and each time the network is pruned some percentage of the elements in the mask are switched to 0 based on the magnitude of their associated weight in the learnable matrix. By the end of the last pruning step the mask has exactly enough 1s such that when stored in CSR format the respective non-zero parameters would take up the targeted amount of storage space.

To the programmer, this entire process is transparent and consists only of changing a few function calls to use our library (such as replacing `tf.get_tensor` with `dt.get_tensor`). Furthermore, training works exactly as before, and the optimization functions included with TensorFlow will correctly backpropagate to the learnable parameters within each sub-graph.

Because same-size networks are extremely model-dependent, we do not support that compression method in our library. Instead, the user tells the library to return an uncompressed model, and he or she manually modifies the relevant hyper-parameters until it is satisfactorily compressed. We added this configuration to facilitate comparison with hand-optimized compressed models.

## 5.2 Initialization of Internal Parameters

Our library initializes the learnable parameters of each sub-graph such that the overall distribution of the represented variable (weight matrix elements) is preserved.

For example, for DeepThin-compressed networks, the learnable parameters  $X^f$  and  $W^f$  must be initialized such that entries in the reconstructed matrix  $W_{Q \times R}$  hold initial distributions similar to those of the uncompressed model. To produce reconstructed weights with initial variance  $\sigma^2$ , our initialization scheme is as follows:

- Initialize entries of rank factor  $X^f$  with the same variance,  $\sigma^2$ , as the original weights should have
- Initialize all entries of rank factor  $W^f$  to a variance of  $\frac{1}{r}$  to maintain that  $\sigma^2$  variance through the reconstruction process

The above initialization scheme works since, in neural networks, weights are randomly initialized by a zero-mean distribution. Weight  $w_{j,k}$  in the reconstructed matrix is computed by the following sum:

$$\sum_{i=0}^{r-1} X_{j,i}^f W_{i,k}^f \quad (8)$$

Since  $X_{j,i}^f$  and  $W_{i,k}^f$  are independent random variables with mean of zero, variance of their product equals the product of their variance,  $\frac{\sigma^2}{r}$ . This summed over  $r$  terms results in the target variance of  $\sigma^2$  for  $w_{j,k}$ . Similar calculations are performed to derive initial mean and standard deviations for non-0-mean initialized variables.

## 5.3 Targeting Compressed Sizes

For all compression methods supported by our library, we set a maximum compressed size ratio and had the library automatically calculate the compression parameters that would best achieve that size target.

Note that, because DeepThin imposes a lower-bound on compression rate determined per-matrix based on the matrix’s shape, targeting an overall network compression rate is not as simple as just compressing all learnable parameters to that ratio (as smaller parameters may hit the lower bound before reaching that ratio). To work around this, we utilize a multi-pass approach, where the user first defines the entire computation graph as well as the desired overall compression rate. In this first step, we leave the shapes of compressing sub-graph parameters undeclared, as we do not yet know to what extent we can or wish to compress each parameter. Next, our library attempts to set the sizes of the sub-graph parameters such that all matrices are compressed to the desired compression ratio, keeping track of when matrices reached their lower-bound, and the delta between the desired size and the lower bound. Finally, we attempt to distribute the “overhead”

caused by matrices hitting their lower-bounds (and the small number of non-compressed model parameters) among other matrices which have not yet reached the lower-bound. This approach allows us to very accurately target compressed sizes to the desired maximum size.

Again, the same-size neural network method is model-dependent and was thus not included in our library. Instead, we hand-tuned the number of hidden units to roughly match the size of the other compression methods. Note that for networks more complex than simple feed-forward networks, deciding exactly how to manually reduce network size is a highly involved process, as deep combinations of convolutional, residual, and other layer types often do not have a single parameter which directly controls the network size.

### 5.3.1 Inference

We tested multiple compression methods and find experimentally in Section 6 that our proposed DeepThin compression method results in better accuracy than any competing method. Motivated by these findings, we decided to investigate the performance of DeepThin-compressed networks further by writing a custom kernel for inference (rather than using existing TensorFlow operations) that computes a DeepThin-compressed matrix multiplication directly, without explicitly decompressing the entire weight matrix at once. We hope that such a fused operation will significantly lower runtime memory, compute, and energy usage of the inference phase by fitting the entire model in the compute device’s cache and taking advantage of particular features of the DeepThin compression method to reduce total computation.

Such considerations are extremely important, especially as devices that are storage-constrained enough to need a compressed model are also very likely to be memory-, compute-, or power-constrained as well. Computing such matrix multiplications more efficiently during the inference phase can directly lead to faster experiences and better battery life, two major considerations on mobile devices.

We wrote our operation directly in C++, using MKL [11] for computations and interfacing with the TensorFlow C++ APIs to define our kernel as a valid operation which can be added to a TensorFlow graph as described above. Our operation takes three parameters: the low-rank factors  $X^f$  and  $W^f$ , as well as the layer input to be multiplied. During the training phase, we tested a range of values for  $r$ , and found that  $r = 1$  works either as

well or better than other possible values with regard to accuracy, and as such all future discussion will assume  $r = 1$ .

As demonstrated in Figure 3, we can think of the decompressed weight matrix  $W$  as having copies of  $W^f$  tiled in a column-major fashion throughout the matrix. Each tiled copy of  $W^f$  is scaled by the corresponding scalar in  $X^f$ . The matrix multiplication is computed such that each cell in the output matrix consists of the sum of the dot products between each of the  $X^f$ -scaled copies of  $W^f$  in a single column and the respective slices of the input  $X$ . We consider two major optimizations for the above DeepThin-compressed matrix multiplication.

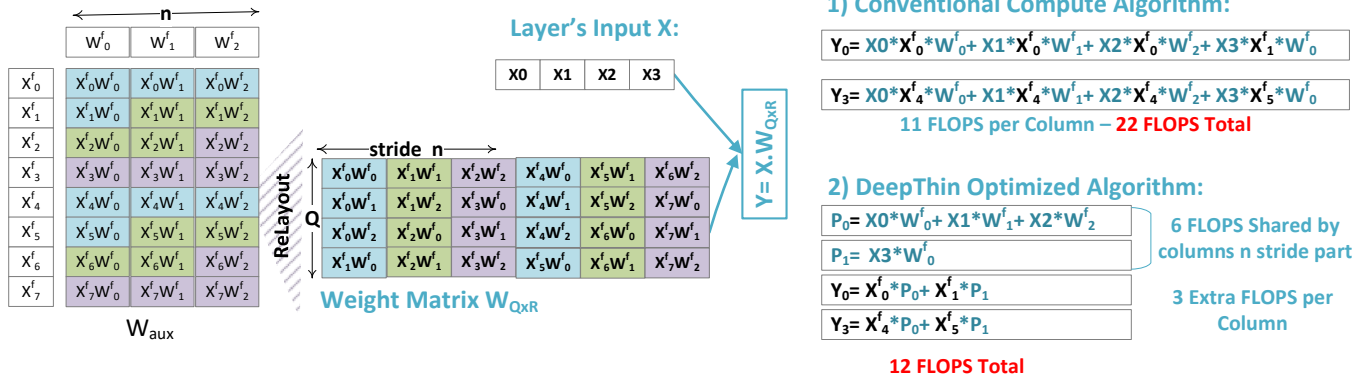
First, instead of scaling each copy of  $W^f$  by an element of  $X^f$  and *then* computing the dot product against the input slice (requiring  $2 \times n$  total multiply-adds), one can *first* compute the dot product between the relevant portions of  $W^f$  and the input slice, then scale the resulting scalar value(s) by the scalar elements of  $X^f$  (requiring  $n + 1$  multiply-adds).

Second, following the above approach, we recognize that at certain points in the computation, shown in Figure 3, we will end up computing the dot product between the same elements of  $W^f$  and the same input slice (although that partial product will be later scaled by different elements from  $X^f$ ). This redundancy can be exploited, such that after the first time a particular  $W^f$  dot product is computed for a particular input slice that dot product is stored, and the kernel scales that dot product by all the  $X^f$  values using it and sums those partial products for all of the cells that make use of that same dot product. This can significantly cut down on the most expensive part of the matrix multiplication, the dot product, by reusing these repetitive computations. Note that the number of times a particular dot product can be reused decreases as the LCM between the  $Q$  and  $n$  dimensions defined in Section 4 increases. Additionally, larger  $R$  dimensions leads to more overall computation, but also more possibilities for reuse.

## 6 Accuracy Results

We compare the accuracy of models compressed with DeepThin for the same compression rate against previous deep compression techniques, which include:

- HashedNet: A small set of possible weight values are distributed into a larger weight matrix according to a hashing function [4].



With  $Q$  and  $n$  being relatively prime, after  $\text{LCM}(n, Q) = n * Q$  entries – every  $n^{\text{th}}$  column of  $W_{Q \times R}$  will be a scaled version of the other. We can exploit this redundancy by factoring out the scale operations – multiplication by  $X^f$  elements.

**Figure 3.** Exploiting redundancy generated by weight compression to optimize computation of  $Y = X * W_{Q \times R}$ .

- Pruning: Matrices are iteratively pruned and the resultant sparse matrices stored with CSR format until the overall size is achieved [9].
- Same-Size Networks: Manually lowering the number of hidden units in a network until the desired size is reached.
- Rank Factorization: Factoring weight matrices into smaller, lower-rank factors [6, 18].

For DeepThin, all networks were compressed with  $r = 1$  and  $n$  calculated as discussed in Section 4. We also compare against DeepThin-Shuffled – a DeepThin-compressed network, where the weight values are randomly distributed throughout the final weight matrix (as opposed to our re-layout operation).

We compared the accuracy of all compression methods on two state-of-the-art speech recognition models. All accuracy plots have had models with a very similar compression rate grouped together horizontally around their mean compression rate in order to increase readability (as each compression method may have its own small differences in the final compressed size). Additionally, rank factorization tends to have a higher lower-bound size than the other methods (due to the requirement that the factor matrices retain dimensions  $Q$  and  $R$ ), and as such have fewer possible configurations.

Although preliminary results show DeepThin accuracy is very competitive on ResNet and other CNN models, We do not report results for CNN models because the unusually large number of input/output channels and activations in modern CNNs would prevent inference models from fitting on the target devices even if

the weights were completely removed (although there is no fundamental limitation of our method).

## 6.1 TFKaldi/Voxforge

First, we evaluated all compression methods on an acoustic model modified from the commonly used open-source speech recognition toolkit TFKaldi [17] and trained on the free Voxforge dataset [1]. The model is a standard feed-forward network consisting of 6 hidden layers of 2048 units each. The inputs to the model are 440 pre-processed audio features, each representing a frame of recorded speech. The outputs of the model are approximately 6928 “phones;” sub-syllable units of speech that are later compiled into words using a grammar-aware beam search decoder (we do not attempt to compress the decoder and do not include it in our size calculations, as it is not part of the deep network). We used the standard Kaldi [15] decoder to decode the phones and calculate word error rate (WER). As is standard in the TFKaldi toolkit, we report the lowest WER result out of a series of test batches.

The TFKaldi model contains 36, 080, 400 parameters and has an application (speech recognition) that is often used on low-power devices, making it a realistic target for compression.

Figure 4 compares the test Word Error Rate (WER) at the end of five training epochs for each compression method compared. As expected, DeepThin networks show better results than competing methods at practically all tested compression rates. The average relative improvement in WER compared to each other method is summarized in Table 1.

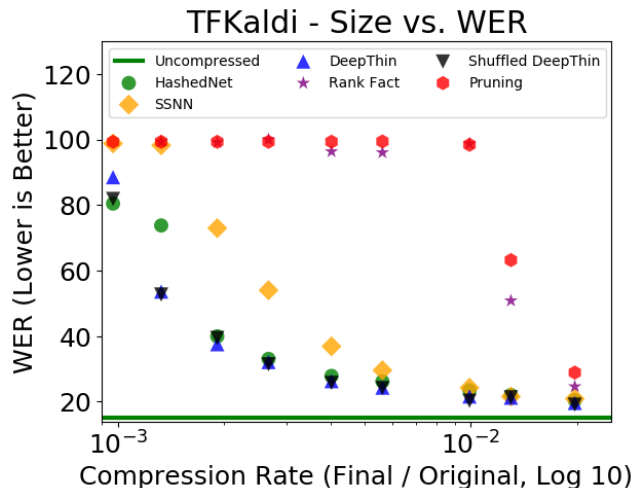


**Figure 4.** Comparing the test word error rate (WER) of different compression methods at a range of compressed sizes for the TFKaldi model. Note that DeepThin models result in lower WERs at all compression rates tested except for the very smallest,  $\frac{1}{1000}$ , configuration, for which HashedNet achieves a lower WER. However, HashedNetworks have prohibitively expensive computational requirements and memory access patterns. Pruning and rank factorization rapidly degrade in performance as the model becomes smaller. Same-size networks perform well, but even with the non-scalable manual effort fail to match our low error rates.

Looking closer at Figure 4, we first compare DeepThin to a same-size network, which represents a hand-tuned reduction in model parameters by reducing the size of each hidden layer in the network. We find that DeepThin consistently outperforms such same-size networks, clearly showing that our method makes more efficient use of its parameters even at such small sizes.

Next, we find that pruned models perform particularly poorly, losing nearly all ability to learn at compressed sizes less than approximately  $\frac{1}{100}$  of the uncompressed network. This can be attributed to the requirement that vast majorities of the model parameters be set to 0 in order to maintain the compression rate under CSR. This gives very little freedom to the network to learn anything at all. The inefficiencies of CSR only exacerbate the problem as the sizes get extremely small, requiring even more parameters to be pruned away than the compression rate would suggest.

The HashedNet model at the very smallest configuration has a slightly lower WER than the corresponding DeepThin networks, however such HashedNet models

require significantly more computation and randomized memory access patterns which are very difficult to optimize for. Additionally, at all other configurations the DeepThin models outperform HashedNet, by up to 2 – 3% absolute WER.

Rank factorization performs very poorly as the size decreases, which is mostly due to the increase in symmetry effects discussed in Section 4 as the rank of the factors decreases to reach a lower compressed size. Solving this symmetry issue with the auxiliary matrix and re-layout operation as described in Section 4 is one of our main contributions, and the improvements from rank factorization to the DeepThin models visible in Figure 4 highlight its success.

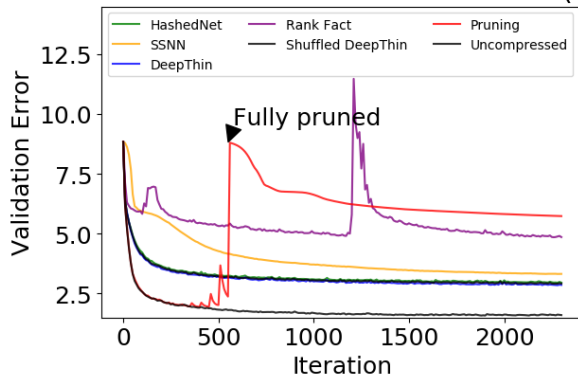
Finally, we see that our method performs very similarly to a “shuffled DeepThin” approach, where  $W_{aux}$  is randomly distributed into  $W$  (thus completely avoiding any symmetries in the final weight matrix). This shows that our re-layout operation, while being significantly more efficient to compute than a random shuffle, is still able to effectively deal with the symmetry issues caused by such factorization methods.

Figure 5 shows the change in validation loss during training for a single compressed size (about  $\frac{1}{250}$  of the uncompressed model). Note that the pruned network (in red) begins training as an uncompressed model, then prunes weights incrementally every 50 iterations until the 550th iteration. As expected, we find that pruning has very little effect on accuracy for the first few pruning iterations, during which time it prunes away almost exclusively unimportant weights that would be essentially 0 even in a dense network. After approximately step 400, however, the prune steps are visible as large jumps in the validation loss, as the network is forced to begin removing weights that are vital to accurately predicting the output classes.

	Rank	Prune	SSNN	Hash
TFKaldi	60.08%	56.96%	23.40%	6.12%
DeepSpeech	28.09%	27.21%	20.45%	12.16%

**Table 1.** Average relative improvement of DeepThin compared to four other compression methods. TFKaldi numbers are in relative WER decrease, while DeepSpeech numbers are in relative test error reduction. Here we see that different compression methods tend to do better on different datasets, however DeepThin consistently beats all other compression methods tested.

TFKaldi - Iteration vs. Validation Error (1-250)



**Figure 5.** Tracking the validation loss for a single compression rate ( $\frac{1}{250}$ ) on the TFKaldi model, compared across the different methods tested. Note that the pruned model is not completely compressed until iteration 550, at which point it trains very poorly. Additionally, we see instability in the training of rank-factored matrices which is removed in the DeepThin curve through the use of the re-layout operation. HashedNets have very similar accuracy results to the DeepThin method, but rely on random memory access patterns and complex hash computations that significantly impede model runtime performance.

This visually demonstrates both how well pruning works for fairly large compressed network sizes (the initial smooth, decreasing portion of the graph where the weights pruned are unimportant) and the negative effects of pruning past this point (when the validation loss begins to increase significantly after each pruning step).

Rank-factorization (simply factoring each  $Q \times R$  matrix into a  $Q \times r$  and  $r \times R$  matrix) is particularly unstable. Multiple times throughout the training process it diverges, and eventually ends up as the second-worst performing model. As the target compressed size gets smaller, we have found that this instability becomes an even larger issue, preventing it from ever reaching a satisfactory convergence better than the initial random parameters. This issue is caused primarily by the symmetries described in Section 4, which motivated and is solved by the use of an auxiliary matrix and re-layout operation in DeepThin.

We see as well that, although the same-size network approach reaches a reasonable validation loss by the end of training, it takes significantly longer to converge than DeepThin or HashedNet-compressed networks,

which is not ideal when training resources are in high demand.

Finally, Figure 5 shows that HashedNets have extremely similar training curves to the DeepThin models, but our DeepThin models ultimately converge to a lower validation loss and WER. Additionally, HashedNets require both the computation of a complex hash and a random memory access for each individual weight in a weight matrix, which can have extreme effects on runtime performance. In contrast, we show in Section 7 that DeepThin has no such issues, and can be highly optimized to run significantly faster than uncompressed models, especially with the product-reuse technique demonstrated in Figure 3.

## 6.2 DeepSpeech

We also tested DeepThin and other discussed compression techniques on a state-of-the-art speech recognition system called DeepSpeech [3]. This model, recently open sourced by Baidu, combines a one-dimensional convolutional layer, multiple GRU recurrent layers [5], and a feed-forward layer to produce a character prediction from a raw frequency spectrum. This system can be trained end-to-end to directly predict text from speech at the character level without a decoder.

We had a number of problems with the open-source model, particularly with its tendency to overfit the limited training data available. To overcome this, and to integrate it with our library, we ported it to TensorFlow, added learning rate decay, and removed batch normalization [12] on the recurrent layers.

The open-source DeepSpeech model contains neither a language model back-end nor any word error rate evaluation code, which prohibits us from reporting model WER. Instead, we report the test loss using the evaluation scripts included with the model.

Figure 6 compares the best test loss after twenty training epochs for each compression method compared on the DeepSpeech model. Here, DeepThin networks outperform all other compression methods at all tested configurations. The average relative improvement in test loss compared to each other method is summarized in Table 1.

Furthermore, Figure 6 shows that pruning performs particularly poorly for this model. We believe that because the model contains a number of smaller matrices, pruned models are forced to prune many layers almost completely, and this issue compounds itself as the input goes through the series of heterogeneous layers, each layer receiving significantly less information.

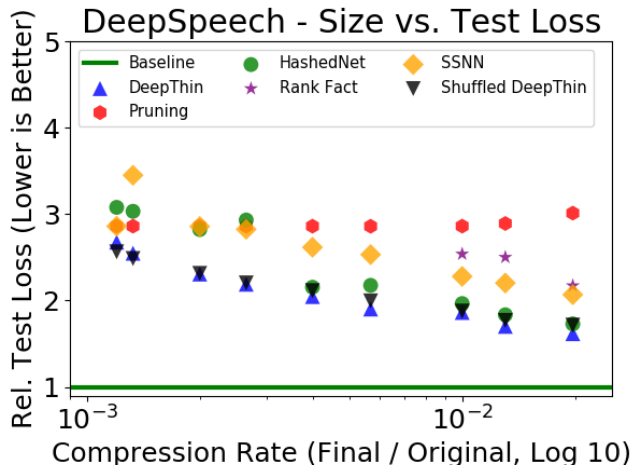


**Figure 6.** Comparing the test loss of different compression methods at a range of compressed model sizes for the DeepSpeech speech recognition model. Note here that DeepThin models significantly outperform all other compression methods, while same-size networks perform well for larger models but fail when the compressed size is made smaller. Pruning, rank factorization, and HashedNets all quickly devolve into ineffective models, only ever predicting the few most common letters (or complete silence) instead of learning useful models.

Same-size models perform competitively when the model size is relatively large, but lose almost all learning capacity as the sizes decreases.

HashedNets are more consistent, and do not lose learning ability as much as same-size or pruned networks, however even at the larger size networks tested they perform worse than DeepThin networks. Coupled with the serious performance and optimization issues encountered with HashedNets, they are clearly not a good choice for this model.

The rank-factorization models, meanwhile, show mediocre results and hit their lower-bound at approximately  $\frac{1}{100}$  the original model size - making them very difficult to compare to other methods and impossible to use for the majority of compression ratios targeted.

Furthermore, as with TFKaldi, we find that our proposed method performs slightly better than a shuffled DeepThin approach. Again, this demonstrates the effectiveness of our re-layout operation in removing symmetry issues while remaining highly efficient to compute. We also expect the non-shuffled DeepThin to do particularly well here, as it can still take advantage of local patterns in the input data that are particularly strong

for the raw frequency spectrum inputs of DeepSpeech compared to the pre-processed features in the TFKaldi model.

### 6.3 LCM Effects

Next, we wanted to compare the effects of the LCM between  $n$  and  $Q$  as discussed in Section 4.

We did this by comparing the same compression rate (approximately  $\frac{1}{100}$ ) on TFKaldi using multiple different  $n$  values, to achieve different LCMs. The result is shown in Figure 7.

Here we can clearly see the positive effect of choosing values for  $n$  that increase the LCM, and find a 28.56% relative decrease in validation loss by increasing the LCM (divided by 2048) from 25 to 101.

However, the trend is not extremely strong - as long as the LCM is not actively *minimized*, it seems that there is some variation in final validation loss given a certain LCM. This is partly because the figure is incomplete - in such a simple experiment, we can only consider the LCM with respect to one set of layers at a time, in this case the majority of the layers which have an input of 2048 units. At the same time, the first layer has 440 input units, which has a different factorization and causes different LCMs with the same values of  $n$ . This means that many of the points have higher or lower LCMs with respect to the input layer than they do with the other layers shown in the figure, causing extra symmetry issues that affect the final validation

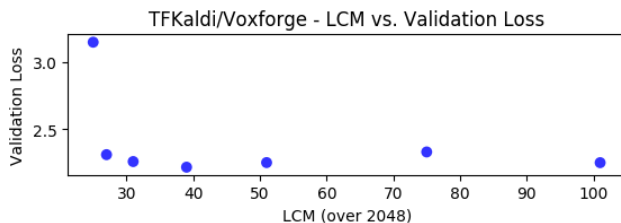


**Figure 7.** Compares the accuracy of a model at multiple LCM values. Note that LCM values are reported with respect to the hidden and output layers that have an input dimension of 2048 units, and the actual LCMs have been divided by 2048 (the largest common factor) to improve readability. Here we see that not optimizing LCM values can cause large accuracy issues, but beyond an initial optimization the trend is less clear. It is clear, however, that maximizing the LCM is a reasonable approach to minimize the validation loss without testing multiple complete configurations and training rounds.

loss which are not accounted for in the figure. This highlights the importance of choosing a different  $n$  for each layer with a different input dimension  $Q$  in order to maximize the LCM on a per-layer basis, which our library is able to do automatically.

Additionally, we believe that the association between higher LCM and lower validation loss is mostly a rule of thumb - as long as the LCM is reasonably large, further increases impact model capacity to a lesser extent.

## 7 Performance Results

We evaluated the performance of DeepThin inference across three Haswell- and Broadwell-based platforms with varying cache sizes. Both the baseline, uncompressed implementations and DeepThin leverage MKL. The first platform is a Broadwell machine (CONF1) with 4 cores/8 threads at 3.30 GHz, 1 memory channel, and 6 MB of L3 cache. Next, we have a Broadwell-E machine (CONF2) with 10 cores/20 threads at 3.00 GHz, 8 memory channels, and 25 MB of L3 cache. Finally, the third platform is a Haswell machine (CONF3) with 36 cores/72 threads running at 2.30 GHz, 16 memory channels, and an L3 cache of 45 MB. All machines had 32 KB of L1 and 256 KB of L2 cache, and all tests were run on the CPU only.

We were particularly interested in how much faster our DeepThin models are when compared to the original, uncompressed model. To test this, we ran 1,000 one-batch iterations through the uncompressed TFKaldi DNN, and 100 one-batch iterations through the uncompressed DeepSpeech network (DeepSpeech is a considerably slower network, so we ran fewer batches). After recording the time taken, we ran the same tests on DeepThin-compressed versions of each model using the custom TensorFlow operation described in Section 5.3.1 and optimized to compute directly on the low-rank factors  $X^f$  and  $W^f$ . We report the speedup (X) for each configuration in Table 2.

Table 2 clearly demonstrates the impressive performance gains realizable from using DeepThin, sometimes reaching speeds of up to 14X faster than the uncompressed model. This effect is primarily visible on the machine equipped with smaller caches that more closely represents a real-world lower-end client situation, though we also find large performance benefits on even the most capable, cluster machine.

Most of these performance gains come from a smaller overall memory footprint that often results in the entire model being stored in the CPU cache(s), significantly

~Rel. Size	TFKaldi			DeepSpeech		
	CONF1	CONF2	CONF3	CONF1	CONF2	CONF3
0.0195	3.80X	2.51X	2.46X	7.66X	2.24X	2.08X
0.0129	5.64X	3.16X	3.51X	10.66X	3.09X	2.77X
0.0099	6.47X	3.88X	4.09X	12.12X	3.50X	3.09X
0.0057	8.12X	4.21X	4.84X	13.69X	3.89X	3.67X
0.0040	8.53X	5.69X	5.32X	13.72X	3.86X	3.70X
0.0027	8.22X	5.22X	5.42X	13.04X	3.65X	3.46X
0.0020	7.43X	4.56X	4.58X	11.68X	3.36X	3.22X
0.0014	4.44X	4.12X	2.44X	8.72X	2.57X	2.42X

**Table 2.** Comparing the execution speed of DeepThin models across both TFKaldi and DeepSpeech at a range of different compressed sizes and machines. Compressed sizes have small variations between machines, but are accurate within 0.0001. All results are presented in "X faster" than the speed of the uncompressed, baseline model. We find that the largest gains come from platforms with smaller cache sizes, but that using DeepThin consistently reduces execution time across all configurations tested, making it ideal for environments where latency and power usage are important.

improving performance over multiple runs, as it no longer has to wait to receive model parameters from the slower main memory.

However, a smaller memory footprint alone is not enough - models like HashedNet, for example, have similarly small memory usage but require the computation of an expensive hash function and a random, non-contiguous memory access to compute the matrix multiplication. DeepThin, by contrast, requires no such hashing function and uses completely contiguous memory accesses. Furthermore, as discussed in Section 5.3.1, DeepThin models can be further optimized for inference performance by re-using partial products, which can cut the amount of computation by over 2X in some models.

Note that the trend in the table is that smaller models run faster, up to about 0.0027 of the original model size. However, once the model is small enough to fit in a sufficiently-fast cache, the most important factor in the models speed quickly becomes how often the dot products can be reused, as shown in Figure 3. As the models get smaller,  $n$  must increase (see Equation 7 -  $n$  is usually much smaller than  $Q \times R$ , making the first term in the numerator - which shrinks as  $n$  increases - the most important in determining compression rate), which means there are fewer total partial products and

a larger LCM, allowing for less total reuse in the computation and thus more overall computation.

## 8 Conclusions

Compressing machine learning models to run on storage-, compute-, and power-constrained devices is quickly becoming a major area of research and industry interest. Existing compression methods struggle to compress models below 1 – 2% of their original sizes and/or add significantly to the computational complexity of the models. We propose DeepThin, a compression method improving significantly on low-rank matrix factorization. We also present a compression library that integrates with TensorFlow to quickly and easily compress machine learning models with multiple compression methods. We evaluate DeepThin and find that it achieves up to 60% better results than competing methods. Finally, we devise a custom kernel for DeepThin-compressed networks and demonstrate inference speed increases of up to 14X over uncompressed networks using a variety of performance optimizations.

## References

- [1] August 2017. VoxForge English Corpus. (August 2017). <http://www.repository.voxforge1.org/downloads/SpeechCorpus/Trunk/Audio/Main/>
- [2] Martín Abadi, Ashish Agarwal, Paul Barham, Eugene Brevdo, Zhifeng Chen, Craig Citro, Greg S. Corrado, Andy Davis, Jeffrey Dean, Matthieu Devin, Sanjay Ghemawat, Ian Goodfellow, Andrew Harp, Geoffrey Irving, Michael Isard, Yangqing Jia, Rafal Jozefowicz, Lukasz Kaiser, Manjunath Kudlur, Josh Levenberg, Dan Mané, Rajat Monga, Sherry Moore, Derek Murray, Chris Olah, Mike Schuster, Jonathon Shlens, Benoit Steiner, Ilya Sutskever, Kunal Talwar, Paul Tucker, Vincent Vanhoucke, Vijay Vasudevan, Fernanda Viégas, Oriol Vinyals, Pete Warden, Martin Wattenberg, Martin Wicke, Yuan Yu, and Xiaoqiang Zheng. 2015. TensorFlow: Large-Scale Machine Learning on Heterogeneous Systems. (2015). <https://www.tensorflow.org/> Software available from tensorflow.org.
- [3] Dario Amodei, Sundaram Ananthanarayanan, Rishita Anubhai, Jingliang Bai, Eric Battenberg, Carl Case, Jared Casper, Bryan Catanzaro, Qiang Cheng, Guoliang Chen, Jie Chen, Jingdong Chen, Zhijie Chen, Mike Chrzanowski, Adam Coates, Greg Diamos, Ke Ding, Niandong Du, Erich Elsen, Jesse Engel, Weiwei Fang, Linxi Fan, Christopher Fougner, Liang Gao, Caixia Gong, Awni Hannun, Tony Han, Lappi Johannes, Bing Jiang, Cai Ju, Billy Jun, Patrick LeGresley, Libby Lin, Junjie Liu, Yang Liu, Weigao Li, Xiangang Li, Dongpeng Ma, Sharan Narang, Andrew Ng, Sherjil Ozair, Yiping Peng, Ryan Prenger, Sheng Qian, Zongfeng Qian, Jonathan Raiman, Vinay Rao, Sanjeev Satheesh, David Seetapun, Shubho Sengupta, Kavya Srinet, Anuroop Sriram, Haiyuan Tang, Liliang Tang, Chong Wang, Jidong Wang, Kaifu Wang, Yi Wang, Zhijian Wang, Zhiqian Wang, Shuang Wu, Likai Wei, Bo Xiao, Wen Xie, Yan Xie, Dani Yogatama, Bin Yuan, Jun Zhan, and Zhenyao Zhu. 2016. Deep Speech 2 : End-to-End Speech Recognition in English and Mandarin. In *Proceedings of The 33rd International Conference on Machine Learning (Proceedings of Machine Learning Research)*, Maria Florina Balcan and Kilian Q. Weinberger (Eds.), Vol. 48. PMLR, New York, New York, USA, 173–182. <http://proceedings.mlr.press/v48/amodei16.html>
- [4] Wenlin Chen, James T. Wilson, Stephen Tyree, Kilian Q. Weinberger, and Yixin Chen. 2015. Compressing Neural Networks with the Hashing Trick. In *Proceedings of the 32Nd International Conference on International Conference on Machine Learning - Volume 37 (ICML'15)*. JMLR.org, 2285–2294. <http://dl.acm.org/citation.cfm?id=3045118.3045361>
- [5] Kyunghyun Cho, Bart Van Merriënboer, Dzmitry Bahdanau, and Yoshua Bengio. 2014. On the Properties of Neural Machine Translation: Encoder–Decoder Approaches. *Proceedings of SSST-8, Eighth Workshop on Syntax, Semantics and Structure in Statistical Translation* (2014). <https://doi.org/10.3115/v1/w14-4012>
- [6] Misha Denil, Babak Shakibi, Laurent Dinh, Marc' Aurelio Ranzato, and Nando de Freitas. 2013. Predicting Parameters in Deep Learning. In *Advances in Neural Information Processing Systems 26*, C. J. C. Burges, L. Bottou, M. Welling, Z. Ghahramani, and K. Q. Weinberger (Eds.). Curran Associates, Inc., 2148–2156. <http://papers.nips.cc/paper/5025-predicting-parameters-in-deep-learning.pdf>
- [7] David Ha, Andrew Dai, and Quoc Le. 2016. HyperNetworks.
- [8] Song Han, Huizi Mao, and William J Dally. 2016. Deep Compression: Compressing Deep Neural Networks with Pruning, Trained Quantization and Huffman Coding. *International Conference on Learning Representations (ICLR)* (2016).
- [9] Song Han, Jeff Pool, John Tran, and William Dally. 2015. Learning both Weights and Connections for Efficient Neural Network. In *Advances in Neural Information Processing Systems (NIPS)*. 1135–1143.
- [10] David A. Huffman. 1952. A Method for the Construction of Minimum-Redundancy Codes. *Proceedings of the IRE* 40, 9 (1952), 1098–1101.
- [11] Intel. 2017. Intel Math Kernel Library. (2017). <https://software.intel.com/en-us/mkl>
- [12] Sergey Ioffe and Christian Szegedy. 2015. Batch Normalization: Accelerating Deep Network Training by Reducing Internal Covariate Shift. *international conference on machine learning* (2015), 448–456.
- [13] Max Jaderberg, Andrea Vedaldi, and Andrew Zisserman. 2014. Speeding up Convolutional Neural Networks with Low Rank Expansions.. In *British Machine Vision Conference 2014*.
- [14] Bo Li, Tara Sainath, Arun Narayanan, Joe Caroselli, Michiel Bacchiani, Ananya Misra, Izhak Shafran, Hasim Sak, Golan Pundak, Kean Chin, Khe Chai Sim, Ron J. Weiss, Kevin Wilson, Ehsan Variani, Chanwoo Kim, Olivier Siohan, Mitchel Weintraub, Erik McDermott, Rick Rose, and Matt Shannon. 2017. Acoustic Modeling for Google Home. [http://www.cs.cmu.edu/~chanwook/MyPapers/b\\_li\\_interspeech\\_2017.pdf](http://www.cs.cmu.edu/~chanwook/MyPapers/b_li_interspeech_2017.pdf)
- [15] Daniel Povey, Arnab Ghoshal, Gilles Boulianne, Lukas Burget, Ondrej Glembek, Nagendra Goel, Mirko Hannemann, Petr Motlicek, Yanmin Qian, Petr Schwarz, Jan Silovsky, Georg

- Stemmer, and Karel Vesely. 2011. The Kaldi Speech Recognition Toolkit. In *IEEE 2011 Workshop on Automatic Speech Recognition and Understanding*.
- [16] Russell Reed. 1993. Pruning algorithms-a survey. *IEEE Transactions on Neural Networks* 4, 5 (1993), 740–747.
- [17] Vincent Renkens. May 2017. Train a tensorflow neural net with kaldi alignments as targets. (May 2017). <https://github.com/vrenkens/tfkaldi>
- [18] Tara N. Sainath, Brian Kingsbury, Vikas Sindhwani, Ebru Arisoy, and Bhuvana Ramabhadran. 2013. Low-rank matrix factorization for Deep Neural Network training with high-dimensional output targets. *2013 IEEE International Conference on Acoustics, Speech and Signal Processing* (2013), 6655–6659.
- [19] R.A. Snay. 1976. Reducing the profile of sparse symmetric matrices. *Bull. Geodesique* (1976).
- [20] Anthony Weber and Amazon Alexa. 2016. *Amazon Echo: The Best User Guide to Master Amazon Echo Fast*. CreateSpace Independent Publishing Platform, USA.